JOURNAL OF APPLIED ELECTROCHEMISTRY 14 (1984) 39–46

Thermal properties of sodium–sulphur cells

REINHARD KNÖDLER

Brown, Boveri and Cie AG, Central Research Laboratory, Eppelheimer Str. 82, 6900 Heidelberg, FRG

Received 28 January 1983

The heat capacity and the rate of heat generation of Na/S cells during discharge and charge were determined. The measurements were carried out in a furnace with very low heat loss and low heat capacity (quasi-adiabatic arrangement). A linear relationship between $(1/I)(dT/dt)$ and I, where I is the discharge or charge current and dT/dt the temperature gradient, was obtained. From these plots the heat capacity of the cell and the entropy term could be determined. It turned out that, due to a steep entropy increase beyond about 80% state of discharge, the heat generation rate increased strongly in this region. During charging, this effect causes a cooling effect at low currents. The data presented here are important for the design of the thermal management system of an electric vehicle battery.

1. Introduction

It is well known, that batteries evolve heat during discharge and charge. This is due to irreversible (polarization) and reversible (entropy change) losses. The rate of heat generation was measured at first in conventional, room temperature systems such as lead–acid and nickel–cadmium [1, 2]. Now data are also available for the high temperature LiAl/FeS battery [3]. Theoretical considerations of heat generation and heat propagation during operation of room-temperature batteries showed that they are in agreement with experiments [4, 5]. The knowledge of the thermal properties of high performance batteries is essential for the dimensioning of the cooling equipment.

Cooling of these batteries during rapid discharge has become a necessity since it was possible to build battery insulations with very low heat losses [6].

The present paper deals with the determination of the heat capacity and the heat generation rate of sodium–sulphur cells as they are developed by Brown, Boveri [7]. In experiments, the adiabatic and the isothermal procedure can be applied. Isothermal measurements are possible only at low discharge rates. They were used previously for the LiAl/FeS system [8]. The experimental set-up is rather complex and will be even more so if the cylinder-shaped sodium–sulphur cells are used instead of the prismatic LiAl/FeS cells. Such an arrangement is in construction at present in our laboratory. Adiabatic measurements can be made only at high discharge rates and require the knowledge of the heat capacity of the cell. The principle of this procedure is to operate a cell in a furnace with very low heat loss and low heat capacity. This guarantees that the heat generated in the cell during operation will remain in the cell itself. Thus, the heat generation rate $\dot{Q}$ can be calculated as the product of heat capacity and temperature change per unit time:

$$\dot{Q} = mc\frac{dT}{dt}. \quad (1)$$

If the measuring time and thus the temperature rise is kept low, dT/dt will be constant and $\dot{Q}$ can be determined rather precisely. In the following, measurements on standard cells using this procedure are presented.

2. Experimental details

A furnace with a vacuum-multifoil insulation was built, which exhibits a low heat loss rate and a small heat capacity. Figure 1 shows the principal features. In order to reduce the heat loss through the current feedthroughs, conventional insulation was wrapped around the leads outside the furnace. About 30 aluminium foils, separated by glassfibre layers ("Superisolierung Doppelschichtsystem",

0021–891X/84 $03.00 + .12.

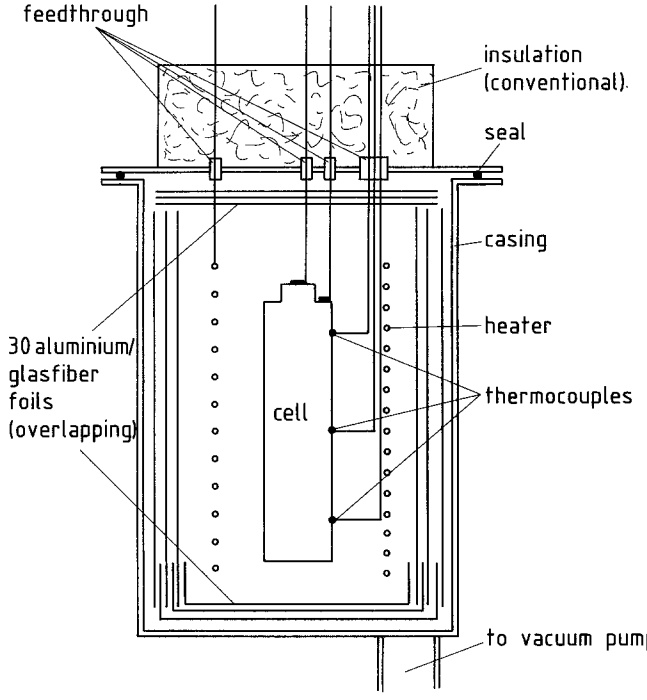

Fig. 1. Quasiadiabatic arrangement for measurement of the heat generation rate of Na/S cells.

Linde AG, Höllriegels Kreuth, W. Germany) were used inside at the wall, the bottom and the lid. The overlapping of the foils was done in such a way that thermal bridges to the casing were avoided. At a vacuum of about 2×10^{-6} bar and a temperature of 330° C, the total heat loss was only 36 W. The outside of the 0.6 m^2 surface of the furnace remained at room temperature. Most of the heat loss was due to the feed-throughs of current, voltage, heater and thermocouples. This effect, which can hardly be avoided, is reflected by the cell's vertical temperature gradient of about 4° C. A low heat capacity of the furnace was achieved by using only the light aluminium foils

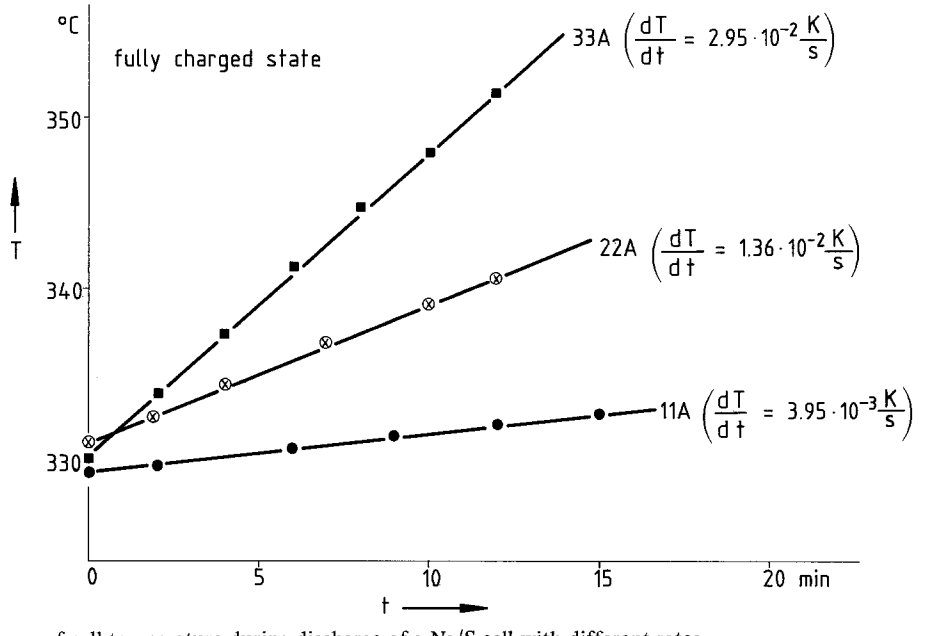

Fig. 2. Incerase of cell temperature during discharge of a Na/S cell with different rates.

and an unsupported heating coil. Thus, an adiabatic behaviour of cells can be expected, at least shortly after starting discharge. Figure 2 shows that the increase of temperature with time at various discharge currents is indeed strictly linear. This proves that the set-up is suitable for measuring the heat rates of cells. The accuracy of dT/dt was estimated to be ± 1.5% for high currents and ± 5% for low currents.

The heat rate was measured at the relatively high discharge and charge currents of about 11, 22 and 33 A (below 10 A the temperature rise becomes too small to be detected accurately). This was done at different states of discharge. The measurement was taken after equilibrium was established (usually one night after changing the state of discharge). The temperature rise was determined during the first 10 to 15 min of discharge or charge (using the thermocouple in the middle of the cell).

Then the state of discharge and the temperature which existed before starting this particular measurement was restored. The starting temperature was about 330° C.

Two Na/S cells out of a standard series were investigated, showing almost the same results. They had a theoretical capacity of 50 Ah and a utilization of about 85%. The d.c. cell resistance in the fully charged state was about 15 to 16 mΩ. This value increased to about 17 to 18 mΩ at higher discharge states (when discharged more than 80%, a further sharp rise was observed). The cell weight was 480 g.

3. Results

The thermodynamic equation for the heat generation $\dot{Q}$ in an electrochemical cell is [4]:

$$\dot{Q} = I\left(\eta - T\frac{dE}{dT}\right) \qquad (2)$$

where I is the current and η the polarization, both taken positive for discharge, negative for charge. $T(dE/dT)$ is the entropy term, being T the absolute temperature and dE/dT the temperature dependence of the open circuit voltage. Determination of dE/dT yielded values between -10^{-4} and $-4 \times 10^{-4}\,V\,K^{-1}$, depending on the state of discharge [9, 10]. In the following, detailed measurements of dE/dT are presented, covering the complete range of discharge states. The (reversible) part $T(dE/dT)$ of Equation 2 becomes most pronounced at low currents, whereas the (irreversible) part η is predominant at high currents. As

$$\eta = IR_z \qquad (3)$$

where R_z is the apparent d.c. cell resistance, the two parts become comparable when $I \approx 3$ A.

Combining Equations 1, 2 and 3 yields:

$$\frac{1}{I}\frac{dT}{dt} = \frac{R_z}{mc}I - \frac{T}{mc}\frac{dE}{dT}. \qquad (4)$$

Therefore, if $(1/I)(dT/dt)$ is plotted against I, straight lines should result with slope R_z/mc and y-axis intercept $(-T/mc)(dE/dt)$. As R_z is known from the difference between open circuit voltage and discharge voltage at a certain current, the heat capacity mc can be obtained from the slope and the entropy can be obtained from the y-axis intercept. Fig. 3 shows that indeed straight lines result when the experimental values of dT/dt (Fig. 2) are plotted according to Equation 4. The slopes increase with increasing discharge state, due to the increasing cell resistance, as mentioned above. A heat capacity of 650 ± 50 $J\,K^{-1}$ can be obtained from the slopes. This value includes all current, voltage and thermocouple connections, so the value of a cell without any attachments will be about 500 $J\,K^{-1}$. Fig. 3 shows also, that the y-axis intercept (i.e. the entropy term) varies with the discharge state. Obviously there is a maximum of $-T(dE/dT)$ at the transition from the two-phase to the one-phase region. At the end of discharge, another steep increase was observed. The entropy term $-T(dE/dT)$ which could be obtained from the y-axis intercepts, is shown in Fig. 4 as a function of the discharge state. The e.m.f. data in this figure were obtained from our own earlier measurements.

Another method for determining the entropy term was applied by using the difference in temperature rise between discharge and charge at the same state of discharge. According to Equation 2, it is

$$\dot{Q}_D - \dot{Q}_C = -2TI\frac{dE}{dT} \qquad (5)$$

where index D stands for discharge and C for charge. The essential point is that the cell resistance does not appear in this equation (provided

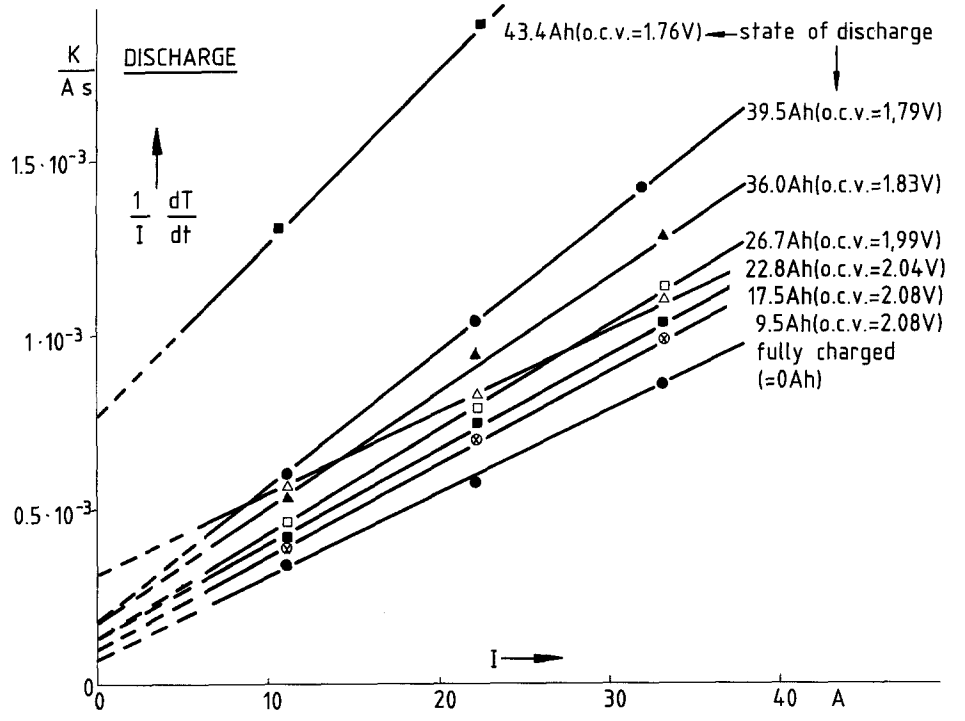

Fig. 3. $(1/I \times dT/dt)$ against discharge current for different states of discharge (values in brackets: open circuit voltage).

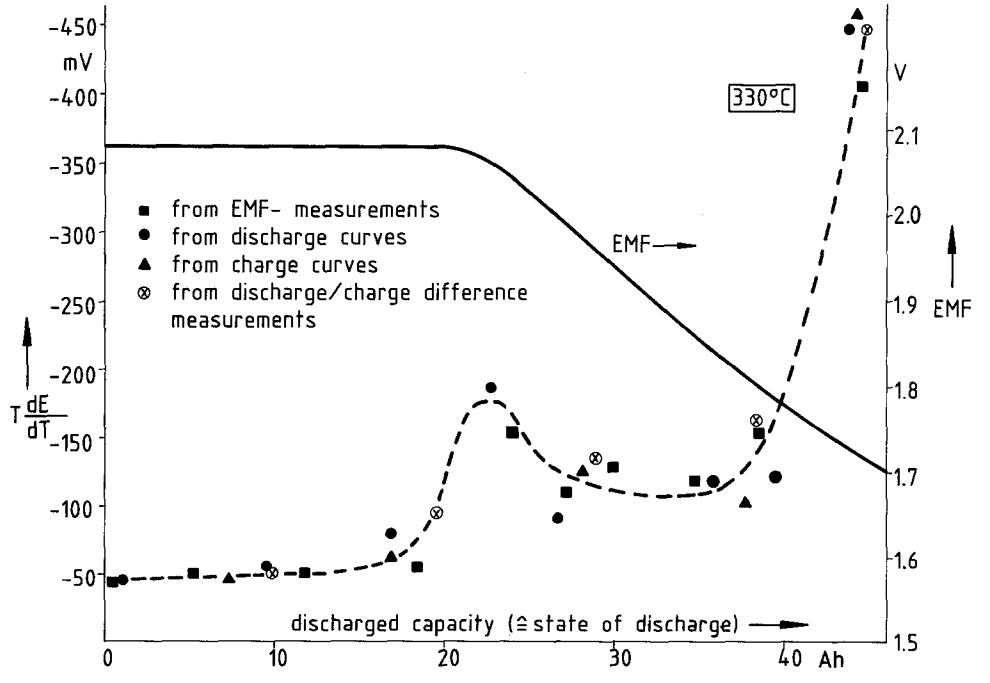

Fig. 4. Entropy term $T(dE/dT)$ against state of discharge as determined by different methods.

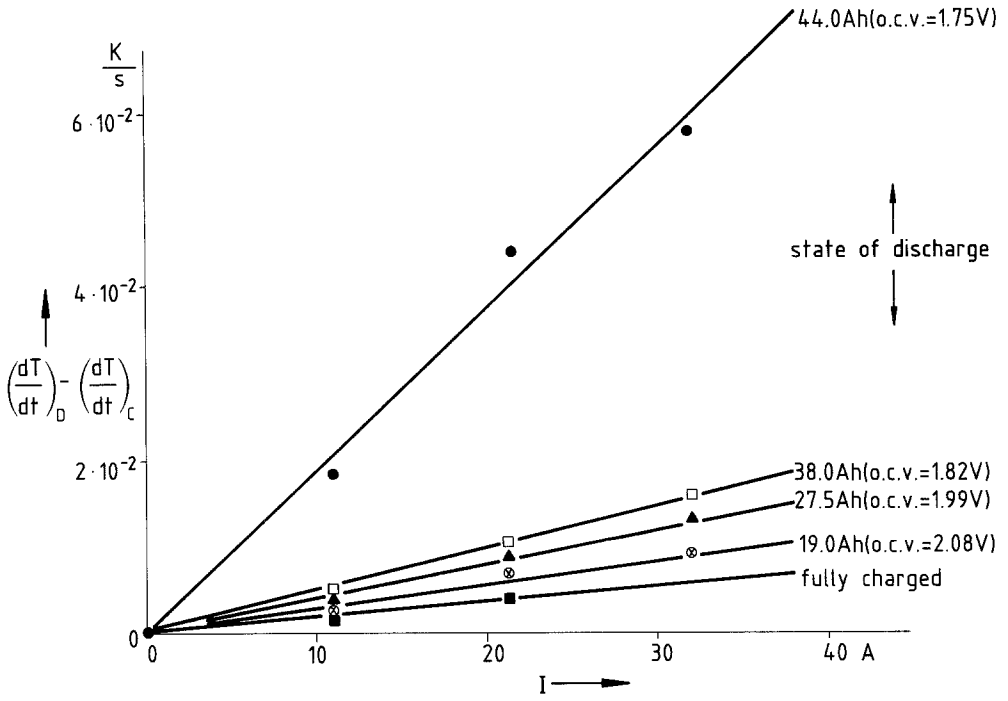

Fig. 5. Difference of the temperature gradients dT/dt between discharge and charge against current for different states of discharge.

that the resistance is the same during charge and discharge, which is usually the case).

Combination of Equation 5 and 1 yields:

$$mc\left[\left(\frac{dT}{dt}\right)_D - \left(\frac{dT}{dt}\right)_c\right] = -2TI\frac{dE}{dT}. \qquad (6)$$

Therefore, a plot of the difference in the velocity of temperature rise during discharge and charge against the current should yield a straight line. Its slope will be proportional to the entropy term $-T(dT/dT)$. Fig. 5 shows that such a linear relationship can indeed be obtained and the values of $T(dE/dT)$ which were obtained from the slopes (crosses in Fig. 4) are in good agreement with those obtained by applying Equation 4.

The rate of heat generation can be calculated by Equation 1, using the measured values of dT/dt at different currents and discharge states. Figures 6 and 7 show plots of the rate of heat generation $\dot{Q}$ during discharge and charge, respectively. It can be seen that at high currents a considerable increase in $\dot{Q}$ during discharge occurs, whereas at low currents a major rise is observed only beyond 40 Ah (about 80% discharge depth). During charge the rate of heat generation is considerably lower than during discharge. In the discharged state at low currents even cooling was observed. Due to the minimum of the entropy term (Fig. 4) $\dot{Q}$ shows a drop in the one-phase region. At high currents this effect is suppressed probably by the high polarization term.

4. Discussion

In contrast to the two-phase region, the scatter in the entropy values in the one-phase region is relatively large (Fig. 4). The reason for this may be the very slow establishment of equilibrium in this region which may even be different for charge and discharge. Nevertheless, the data in Fig. 4 allow a reasonably accurate determination of thermodynamic properties. The changes in the free enthalpy ΔG, the heat of formation ΔH and the entropy ΔS can be expressed as:

$$\Delta G = -zFE \qquad (7)$$

$$\Delta H = -zF\left(E - T\frac{dE}{dT}\right) \qquad (8)$$

$$\Delta S = zF\frac{dE}{dT} \qquad (9)$$

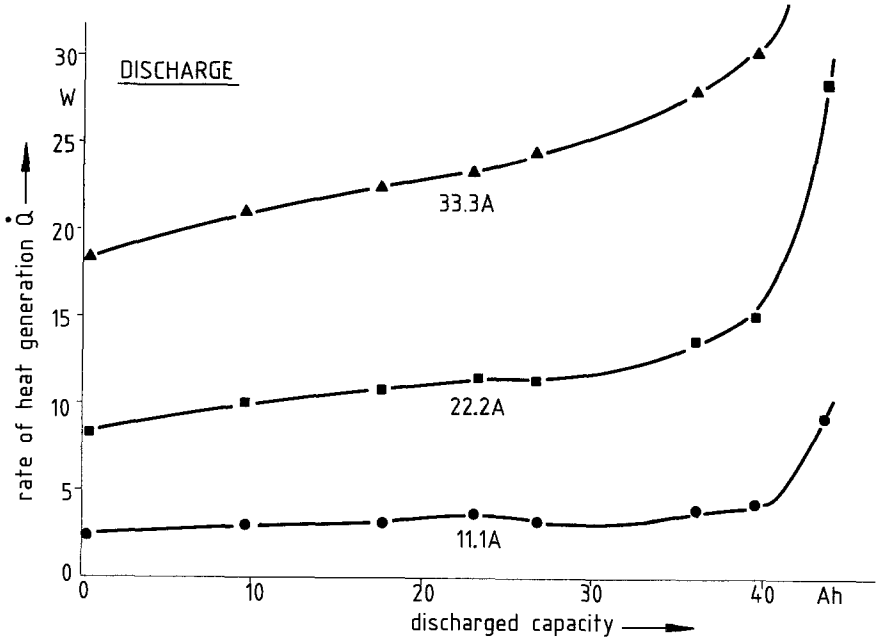

Fig. 6. Rate of heat generation during discharge with different currents. Equilibrium was established at each point before measurement.

where F is the faraday number and z the number of electrons involved in the electrochemical reaction ($z = 2$ in the Na/S cell). In Table 1, values calculated by Equations 7 to 9, using Fig. 4, are listed. There is good agreement with previous work [10], however, the maximum of the (negative) entropy in the transition region and its steep increase in the discharged state is new information. An explanation of this effect, e.g. by a entropy of mixing, requires further investigations and is not being attempted here. In contrast to ΔG, ΔH does not change very much in the course of discharge.

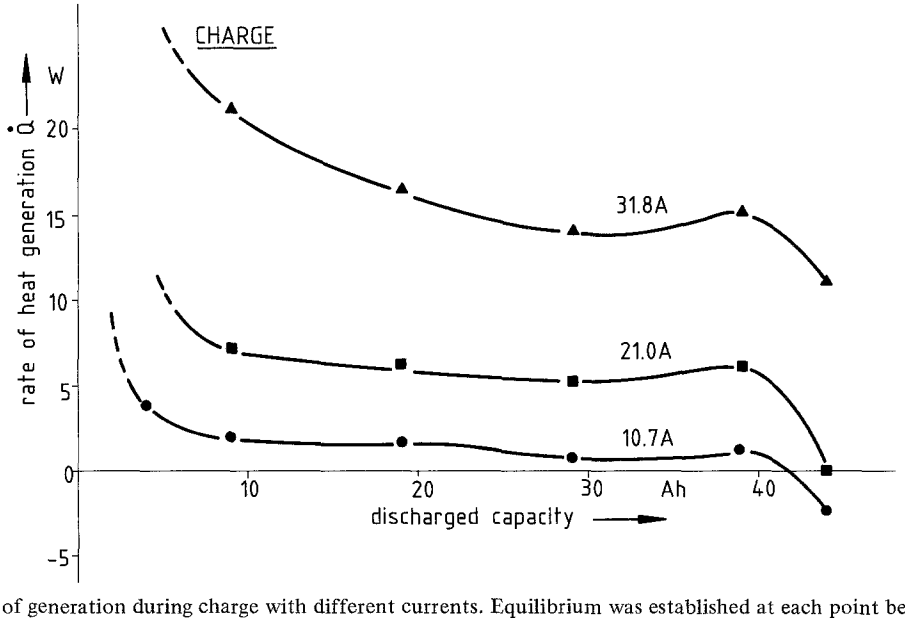

Fig. 7. Rate of generation during charge with different currents. Equilibrium was established at each point before measurement.

Table 1. ΔG-, ΔH-, ΔS-values calculated from the experimental data, using Equations 7, 8, 9

State of discharge	$-\Delta G$ (kJ mol^{-1})	$-\Delta H$ (kJ mol^{-1})	$-\Delta S$ (J mol^{-1} K^{-1})
$E = 2.08$ V: 2-phase region (Na_2S_5 + S)	401 ± 3	410 ± 5	15 ± 3
$E \approx 2.06$ V: transition region between 2-phase and 1-phase region	397 ± 5	430 ± 8	50 ± 8
$E = 1.95$ V: 1-phase region (Na_2S_4)	375 ± 5	398 ± 5	35 ± 6
$E \approx 1.73$ V: deep discharged region (Na_2S_x with $x < 3$)	334 ± 10	420 ± 15	130 ± 20

This means that all components involved in the reaction, like Na_2S_5, Na_2S_4 and Na_2S_2, have similar heats of formation.

The electrical power $\dot{Q}_{el}$ during discharge is described by:

$$\dot{Q}_{el} = (E - R_z I)I. \tag{10}$$

The ratio of heat generation to electrical power can be determined using Equations 2 and 10:

$$\frac{\dot{Q}}{\dot{Q}_{el}} = \frac{T\frac{dE}{dT} + R_z I}{E - R_z I}. \tag{11}$$

For the small currents (i.e. $I \ll (T/R_z)(dE/dT) \approx 3$ A) the ratio becomes constant:

$$\frac{\dot{Q}}{\dot{Q}_{el}} = \text{constant} \approx \frac{T}{E}\frac{dE}{dT}. \tag{12}$$

Thus, in the 2-phase region the rate of heat generation will not fall below about 2% of the electrical power and in the 1-phase region not below about 6%.

The total energy Q_T which is dissipated during discharge can be calculated by:

$$Q_T = \frac{I}{zF}\int_0^T -\Delta H dt \tag{13}$$

$$Q_T = \frac{C}{zF}\int_0^1 -\Delta H dD \tag{14}$$

where $dt = (C/I)dD$, being C the cell capacity and D the discharge depth ($D = 0$ to $D = 1$). Using Equation 8 it is:

$$Q_T = C\left[\int_0^1 E dD - \int_0^1 T\frac{dE}{dT}dD\right]. \tag{15}$$

Thus, the total energy is independent of the cell resistance and the current. Integration over the entire discharge range yields about 2.02 V for the open circuit voltage and about −0.12 V for the entropy term. Thus, the total energy output is:

$$Q_T \approx 2.14C. \tag{16}$$

In an adiabatic system this same energy has to be put into the battery during charging.

In principle there are two ways to operate a battery: in the quasi-adiabatic or the quasi-isothermal mode. The latter is the most common and also the most flexible one. It means heating during the idling periods. In the quasi-adiabatic mode neither cooling nor heating is done and the system maintains its temperature by using the heat generated during discharge and charge. Of course, such an operation mode is restricted to rather low discharge rates and therefore may be applicable only for special cases. In addition, the balance between the heat loss through the insulation and the heat generation rate must be so good that the temperature of the battery will not go below 320° C and not beyond 380° C. The energy efficiency for this operation mode is according to Equation 16:

$$\eta_A = \frac{2.14C}{2.14C + 24H_0} \tag{17}$$

Here a "cycle" of 24 h, consisting of discharge, charge and idle period is being considered. C is the cell capacity (45 Ah) and H_0 the heat loss of a vacuum insulation (about 250 W for the whole battery [6] which means about 0.5 W per single cell). Thus, an efficiency of $\eta_A \approx 89\%$ can be

expected, independent of cell resistance and discharge/charge currents. However, as mentioned above, the currents must counterbalance the heat loss and can therefore be only relatively small. The condition for this balance is:

$$\dot{Q}_D T_D + \dot{Q}_C T_C = 24 H_0 \qquad (18)$$

where $\dot{Q}_D$, $\dot{Q}_C$ are the heat generation rates (discharge, charge) and T_D, T_C the times for discharge and charge, respectively. Using Equation 2, the balance condition will be:

$$CR_z(I_D + I_C) = 24 H_0 \qquad (19)$$

where I_D and I_C are discharge and charge currents, respectively. Taking as an example $R_z = 17\,\text{m}\Omega$ and $I_C = 5.7$ A, which means a 8 h charge, a value of $I_D = 10$ A results, which means a 4.5 h discharge. Thus, an idle period of $T_0 = 11.5$ h remains. Assuming a minimum charge current of 3.7 A (12 h charge), the average maximum discharge current in this mode can be 12 A (3.7 h discharge).

In contrast to the quasi-adiabatic mode, the advantage of the quasi-isothermal mode is that very high discharge currents are allowed. The efficiency of this mode is (valid only for such currents where no heating is necessary):

$$\eta_I = \frac{(2.02 - R_z I_D)C}{(2.02 + R_z I_C)C + T_0 H_0}. \qquad (20)$$

Using the same values as for the quasi-adiabatic mode, an efficiency of $\eta_I \approx 82\%$ results. Thus η_I is clearly smaller than η_A, as expected. If electric vehicle traction is considered, the quasi-isothermal mode will be necessary for a family car with high accelerating capabilities, whereas for a van or a city car the quasiadiabatic mode will be more suitable, offering a higher energy efficiency.

5. Conclusions

The measurements showed that the heat capacity, the entropy term and the heat generation rate of sodium–sulphur cells can be determined by operating them in a furnace with vacuum insulation having low intrinsic heat capacity. Discharge and charge currents should be higher than about 10 A for a 50 Ah cell to ensure sufficient accuracy. It turned out that the negative entropy term is relatively low and almost constant in the two-phase region. In the one-phase region the term is more than twice as large and between these two areas a maximum is observed. Around the melt composition Na_2S_3 a steep increase of the negative entropy term occurs. This behaviour is reflected in the heat generation rate during discharge and charge. At a discharge current of 22 A, e.g. the rate which has increased from about 8 to about 14 W during discharge to 72% of theoretical capacity reaches about 30 W if discharge further to 88%. Therefore, it will be necessary to reduce the power in the deep discharged state. The importance of the entropy term is also shown by the fact that the heat generation rate during discharge is almost twice as high as during charge (at the same current). The data obtained in the course of this investigation are useful for the thermal management of the sodium/sulphur battery. Additional information will come from the planned experiments with an isothermal calorimeter according to [8].

Acknowledgements

This work has been supported by the Bundesministerium für Forschung und Technologie (reference ET-4496 A). I would like to thank H. Reiss for help in the design of the insulation, G. Prappacher and K. Liebermann for experimental assistance.

References

[1] S. Gross, *Energy Conversion* 9 (1969) 55.
[2] K. W. Choi and N. P. Yao, *J. Electrochem. Soc.* **125** (1978) 1011.
[3] H. F. Gibbard, D. M. Chen and T. W. Olszanski, Proceedings of the 16th IECEC (1981).
[4] H. F. Gibbard, *J. Electrochem. Soc.* **125** (1978) p. 353.
[5] C. C. Chen and H. F. Gibbard, Proceedings of the 14th IECEC (1979) p. 725.
[6] R. Knödler and H. Reiss, *J. Power Sources* **9** (1983) 11.
[7] W. Fischer, *Solid State Ionics* (1981) 413.
[8] L. D. Hansen, R. H. Hart, D. M. Chen and H. F. Gibbard, *Rev. Sci. Instrum.* **53** (1982) 503.
[9] B. Cleaver and A. J. Davies, *Electrochim. Acta* **18** (1973) 733
[10] N. K. Gupta and R. P. Tischer, *J. Electrochem. Soc.* **119** (1972) 1033